2 2 2 5 4

UCRL-JC-125975
PREPRINT

Production of Multi-Kilovolt X-Rays from Laser-Heated Targets

C.A. Back
J. Grun
C.D. Decker
J.L. Davis
O.L. Landen
L.J. Suter
R. Wallace

This paper was prepared for submittal to the
Society of Photo-Optical Instrumentation Engineers Annual Meeting
EUV, X-Ray and Gamma-Ray Instrumentation for Astronomy VIII
San Diego, CA
July 27-August 1, 1997

July 1997

Lawrence Livermore National Laboratory

DISCLAIMER

Production of multi-kilovolt X-rays from laser-heated targets

C. A. Back, J. Grun[#], C. D. Decker, J. L. Davis[+], O. L. Landen, L. J. Suter, and R. Wallace

Lawrence Livermore National Laboratory, P. O. Box 808, Livermore, CA 94551
[#]Naval Research Laboratory, 4555 Overlook Ave, SW, Washington, D.C.20375
[+]Alme Associates, Alexandria, VA USA

ABSTRACT

Experiments to develop high photon energy x-ray sources were carried out on the Nova laser. Ten laser beams delivered approximately 39 kJ of energy in 2 ns into a Be cylinder filled with Xe gas. The conversion efficiency into x-rays $\leq$ 4 keV was measured to be 5 - 15 % , which is the highest measured in this photon regime for laser-produced plasmas. The temporal dependence of the x-ray emission indicates that the bulk of the emission is emitted in the first half of the 2 ns pulse. A set of diagnostics were fielded to image the volume in emission as well as provide spectra to measure conversion efficiency.

Keywords: X-ray production, conversion efficiency, laser-produced plasma, backlight, Xe gas, L-shell emission

1. INTRODUCTION

Laser-produced plasmas are applied both as probes of a sample of interest, such as in absorption spectroscopy or radiology, and as a sources of radiation which heat material. In the first case, the source is passive and ideally does not perturb the sample under consideration. In the second case, the radiation heating is sufficient to perturb the state of the material. For these types of applications, there are three major quantities of importance. The frequency distribution of the x-ray source is important because the application may require a specific wavelength region for monochromatic or a broadband imaging suited to the sample to be studied. The brightness of the source is also a defining quantity because it determines the contrast and constrains the opacity of the sample that can be observed. Finally, the temporal duration is important because the timescale of the probe/source may need to be a short burst to probe atomic kinetics, or a long pulse to irradiate test objects.

Papers on the backlight efficiency of lines sources have investigated sources suitable for radiography of laser-fusion targets.[1-6] In these experiments the conversion efficiency was studied as a function of laser wavelength, laser intensity, and temporal duration. The targets are typically solid targets which produce emission from K-shell or L-shell of mid- to high-Z targets (Al through Ti). There have also been studies specific to lithography applications which focus on emission in the 0.8 to 1.2 keV regime. [7 8] More recently, gas-filled targets have been proposed as a candidate for high efficiency x-ray production in the multi-kilovolt range (> 4 keV) .[9] These targets are designed to provide a debris-less source of hard x-rays that can be used to heat large volumes and perform irradiation of large test objects. These sources are also of interest for radiation transfer studies since an efficient broadband source can be tailored by the use of filters to tailor the drive spectrum. With the laser energy that will be available at the National Ignition Facility, we will be able to attain even higher photon energies and longer duration pulses for different applications.

Typical disk targets have limited conversion efficiency because the conditions for the production of multi-keV x-rays are difficult to sustain. In the ablation front where the density is high , the temperature is too low for efficiently generating hard x-rays. In the corona where the laser energy is absorbed, the temperature is much hotter but the plasma density is too low. The design for these experiments is to heat a large volume by a "bleaching" ionization front which creates sufficiently hot and dense plasma to produce a long duration multi-keV x-ray pulse. The targets are Be hohlraums, cylinders with end caps, filled with a gas that generally remains below the critical density of the laser and thus allows good penetration of the laser. To achieve high conversion efficiency, we depend on rapid ionization of the gas, and subsequent compression of the gas by the wall enclosure. In the first stage, the gas ionizes and emits radiation characteristic of the highly ionized species from bound-bound and bound-free transitions. In this stage, the target is very similar to the gas bag targets that have been investigated for laser-plasma studies. However, when the gas is confined in a low Z enclosure the ablation of the wall material compresses the gas and the increased density can lead to a second peak in the x-ray emission and late in time will be quenched by three-body recombination. For these targets, a low Z hohlraum material is chosen to allow the hard x-rays pass through the confining wall with minimal attenuation.

Gas targets created by irradiating thin CH membranes that were filled with gas showed that the conversion efficiency could be up to 6 %.[10] However, the temporal duration of these targets is limited by the disassembly of the CH membrane and subsequent expansion of the gas. The time scale for expansion limits the emission of multi-keV x-rays to a 1.5 ns temporal duration. The goal of these experiments was to enhance the x-ray conversion and duration of the x-ray pulse.

2. EXPERIMENTAL SETUP

Experiments have been performed using the Nova laser which delivered 38- 42 kJ of 0.35 μm laser light in 2 ns flat-topped intensity profile. The targets were Be cylinders that had 100 μm thick walls and 50 μm thick endcaps. The physical dimension of the target is 1.6 mm long and 2.0 mm in diameter. The laser entrance holes (LEH) are 1 mm in diameter and are covered with a thin 0.6 μm thick polyimide windows (($C_{14}H_6N_2O_4$) which confine the Xe gas. This wall material is of low Z and therefore provides little attenuation for the emission above 2 keV, but does significantly attenuate lower photon energies. The laser beams enter through the holes in the endcaps of the target and irradiated the inside of a Be cylinder that was filled with Xe gas. The lasers heat the gas to form a highly ionized plasma which emits x-rays. The x-rays pass through the walls of the Be cylinder and are detected by both time-resolved and time-integrated diagnsotics.

The emphasis for these measurements was the photon energy region above 4 keV where the transmission is 85% or greater. The low Z wall material of the target was designed to produce a tamping effect that would prolong emission of hard x-rays at late times. Figure 1 shows a schematic of the target where the blue regions represent the geometry of the laser beams irradiating the inside walls of the Be cylinder. An actual photograph of the target is also shown in the figure where one can see the endcaps of the enclosure which are glued onto the ends of the cylinder.

schematic cross section of hohlraum

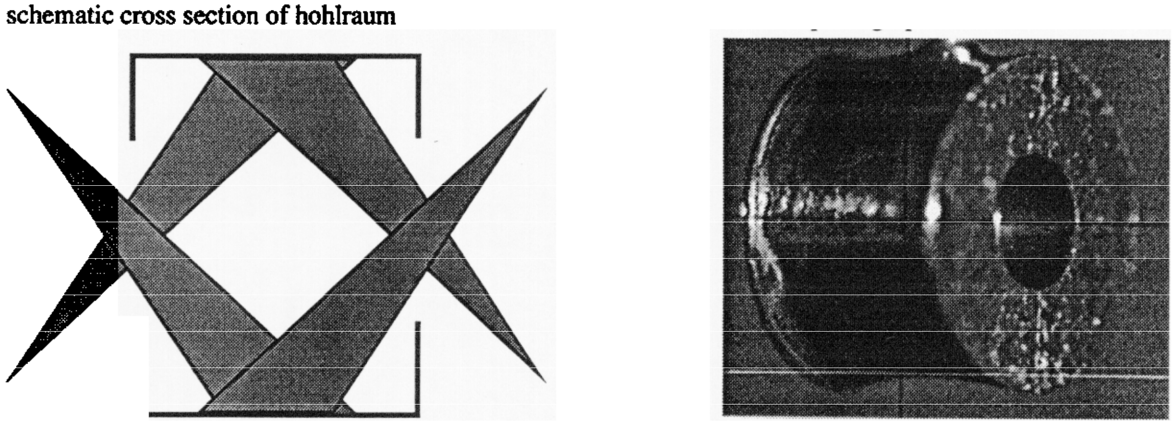

Figure 1. Schematic of laser beam configuration and photograph of the Be cylinder targets. The shaded regions represent the laser beam illumination of the inside of the target. The cylindrical wall of the target was 100 μm thick and the endcaps were 50 μm thick. Thin CH windows covered the laser entrance holes so that the target could be filled with Xe gas.

The primary diagnostic was a time-integrated x-ray diagnostic, the Henway, to obtain absolute measurements on conversion efficiency. It is a Bragg crystal spectrometer coupled to DEF direct x-ray film. Other diagnostics included 2-dimensional x-ray imaging, spatially-resolved gated spectra and streaked spectra. The measurements were performed as a function of Xe gas pressure, 1 atm or 2 atm. In addition, this series of experiments also measured the backscatter to determine whether future experiments would benefit from beam smoothing techniques.

3. EXPERIMENTAL RESULTS

In this series of experiments, conversion efficiency was measured for 1 and 2 atmosphere fill pressures. The same complement of diagnostics were fielded on all shots and the data will be discussed by comparing the data from the two different gas fills.

3.1 X-ray images

Figure 2 shows x-ray pinhole images taken from the side view of the target for 2 different gas pressures. The x-ray images are recorded on a gated microchannel plate and are integrated over approximately 80 ps. The x-rays are filtered by Be and Al to produce images of < 4 keV emission and show the volume of plasma that is contributing to the x-ray emission. At 1.5 ns into the laser pulse, these images show a pronounced plasma plume coming out of the laser entrance holes. The 2-dimensional images are striking because they show a non-uniform heating that was not expected from the design of the target.

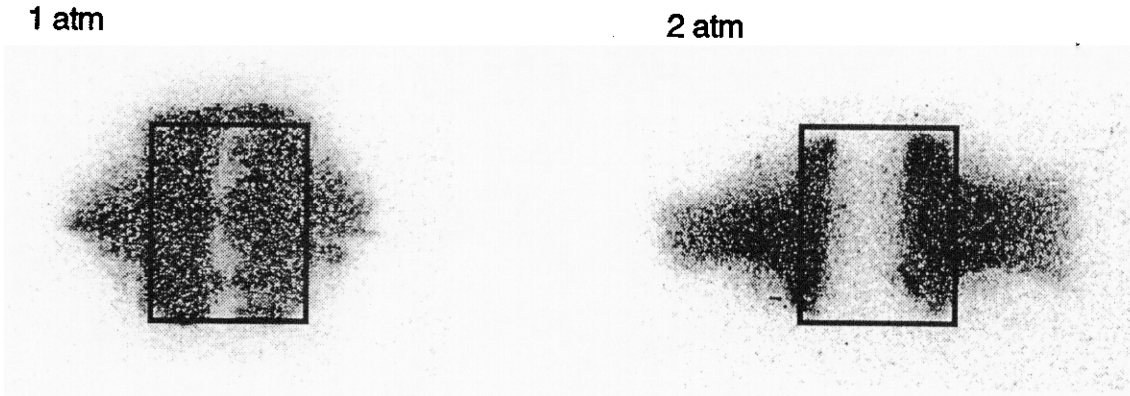

Figure 2. X-ray images of emission above 4 keV at 1.5 ns. The side view of the target is shown on the figure as a rectangular box. The emission from plasma streaming out of the target is quite pronounced at this time.

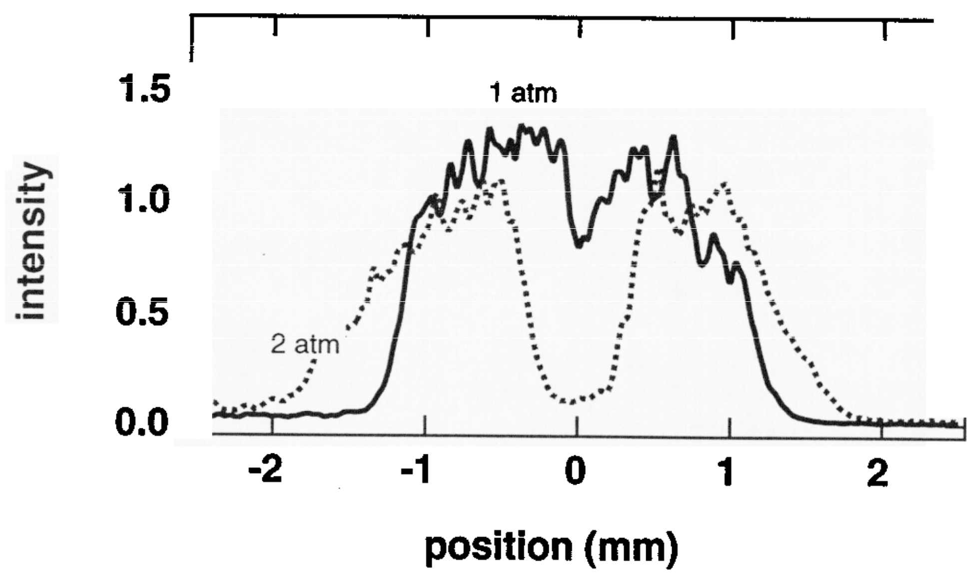

Figure 3 Intensity of the x-ray emission along the length of the cylinder at 1.5 ns. The solid line is data from the 1 atm target, the dotted line is data from the 2 atm target. The outside hohlraum length is ~ 1.8 mm due to the bulge of the CH membranes when they are filled with gas. The emission beyond 0.9 mm is due to the plasma plumes coming out of the laser entrance holes.

The left and right sides of the target are each heated by 5 beams and the images clearly show that two plasma sources are created. The central region of the target is not in emission, even at the end of the laser pulse. Here the plasma is seen to jet out of the laser entrance holes and electron conduction was not sufficient to heat the central region enough to emit > 4 keV x-rays. The data at 1.5 ns of intensity vs. position in figure shows that ~ 500 μm along the axial length of the 2 atm target is not contributing to the emission while only ~250 μm is not in emission for the 1 atm target. Intensity lineouts along the axis are shown in figure 3 where the dotted line is data from the 2 atm target and the solid line is from the 1 atm target. The hohlraum is nominally 1.6 mm long, but since the hohlraum windows which confine the gas bow out ~150 microns the initial length from earlier x-ray images is ~1.8 mm long. In the lineout ,the apparent width is even longer because the plasma outside of the hohlraum is in emission.

Subsequent calculations by Lasnex have suggested that the expansion of the Be near the laser entrance holes interfered with deposition of the laser energy. The beams were deflected enough that the energy deposition remained near the LEH and was no longer directed into the hohlraum and qualitatively a gap in the emission similar to the experimental data is seen. This will be tested in future experiments by the use of a larger LEH.

X-ray images end-on to the cylinder were also obtained and these are shown in figure 4. Here, we compare the results from the two different pressure targets near 500 ps. Since the images are gated, the time the snapshot of the image is obtained is not exactly the same. The 1 atm target shows a clear image of the beam spots on the walls of the Be hohlraum. The spots appear on the inside circumference of the target and the pattern corresponds to the five-fold symmetry of the laser beam irradiation. The 2 atm target at nearly the same time also shows a five-fold symmetry, however, the clear appearance of the spots on the wall is not evident at any time. The ablation of the inside wall of the cylinder produces a Be plasma which is expected to compress the Xe gas. Later images of the 1 atm target show a clear stagnation of the plasma on axis which produces an emission spike at the center. The 2 atm case does not produce a significant spike. These images corroborate the prediction of enhanced density late in time. However, the x-ray emission observed by x-ray streak cameras does not appear to be enhanced due to the compression effect.

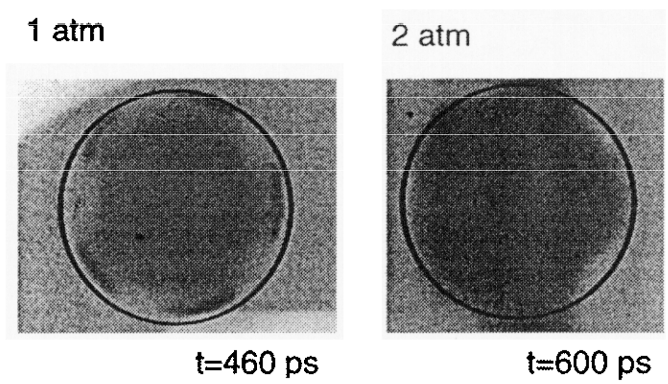

Figure 4. End-on x-ray pinhole images of the target down the hohlraum axis. The outside diameter of the cylinder is overlaid on the images.

3.2 Time-resolved spectrometers

Spectrometers were fielded on the target to provide the temporal history and estimate electron temperature measurements. Spectrometers to record the temporal history were flat rubidum hydrogen phthalate (RAP) crystals coupled to x-rays streak cameras. For electron temperature measurements, a flat pentaerythritol (PET) crystal was coupled to a gated microchannel plate.

The temporal history of the data is obtained on x-ray streak cameras. Calculations of the temporal history are sensitive to the way the electron conduction is modeled in the plasma. These measurements record the temporal shape as well as the duration of the x-ray emission. Figure 5 shows that the emission peaks between 0.5 and 0.8 ns during the 2 ns heating pulse. It significantly dropped during the second half of the pulse. While there are some variations the peak intensity, all shots produced a source which lasted ~ 1 ns. This duration was much shorter than expected from simulations which also predicted a second emission peak due to recompression of the gas along the axis of the hohlraum.

The relative intensities are not absolute. Analyzable data for the 1 atm target was obtained for a shot with only 5 beams. Since the x-ray images show that two nearly independent sources are created by each set of 5 beams, the intensity of the 5 beams in the figure is shown multiplied by a factor of 2. The shape of the temporal profile suggests that for the first 250 ps, the heating is nearly identical for the two targets, but the 1 atm target peaks earlier than the 2 atm target.

An example of the spectrum obtained from the streak camera which views the entire source is shown in figure 6. Another spectrometer gave spatially-resolved spectra that differentiated between the plasma inside the target and the plasma outside of the target. Although these measurements are preliminary, they are encouraging because they show that measurements of plasma conditions will be possible in future experiments. The spectral features of the emission show that the Xe is well ionized past the Nilike ion stage and for the densities expected in these targets, this implies the electron temperature is well above 3.5 keV. Because of the large density gradients in the plasma jetting out of the target, the spectra shows emission from over 5 different ion stages. Emission inside the target saturated the gated spectrometer so a conclusive measurement could not be made. Emission from outside of the target is subject to large density gradients in the plumes and make it impossible to determine a unique plasma temperature. However, based on this data, it is clear that there is enough signal for a spectrometer with higher spatial resolution and future experiments hope to diagnose plasma conditions inside the cylinder.

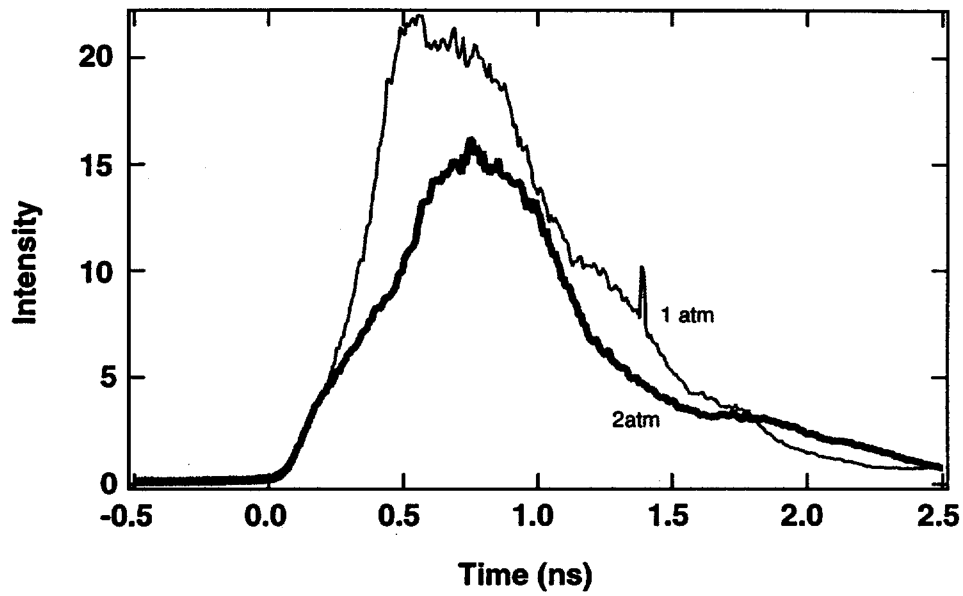

Figure 5. Emission from the n= 2-4 transitions of L-shell Xe (above 4 keV) as a function of time. The laser pulse was 2 ns long.

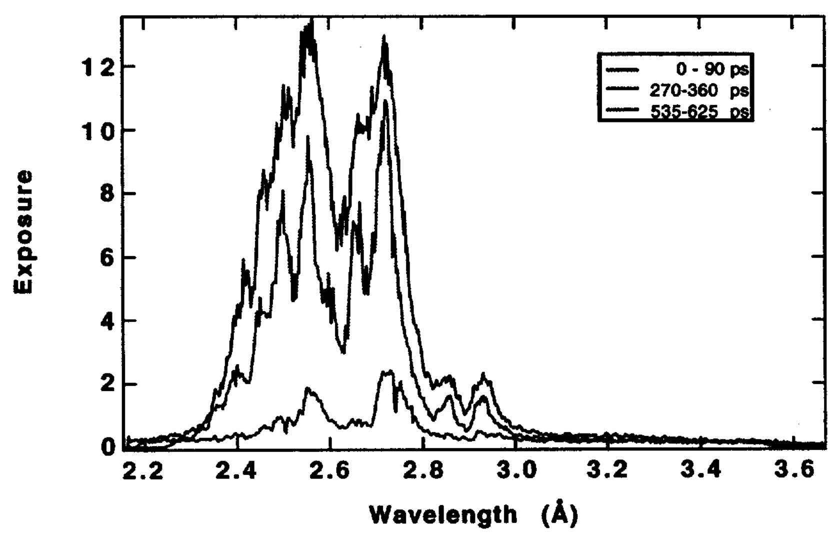

Figure 6. Example of spectra from a highly ionized Xe plasma created by the laser heating the gas inside the Be cylinder. Each lineout is a spectrum taken at different times during the laser pulse.

3.3 Time-integrated spectrometers

The conversion efficiency measurement is obtained from the absolute photon measurements of the Xe emission. An example of this data is shown below in figure 7. This is recorded on a time-integrating Bragg crystal spectrometer and is analyzed by using the Henke crystal calibrations. [11] Data was obtained at two different angles on each shot. One spectrometer viewed down the cylinder axis, while the other viewed the side of the target. The spectrum for each shot is integrated over the photon energy to produce the conversion efficiency of the source. The solid line superimposed on the spectra shows the running integral of the emission.

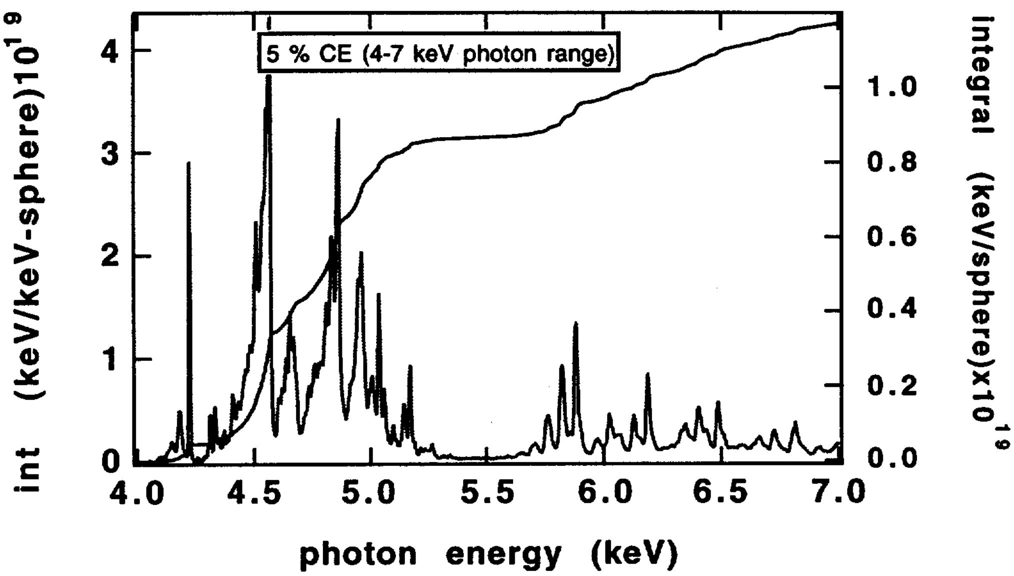

Figure 7. Example of the spectrum obtained from time-integrated Bragg spectrometers. This data integrated of the spectral range to obtain the conversion efficiency measurements.

The spectrum is composed primarily of the n = 2 - 4 and n = 2 - 5 transitions of Xe located in the 4 - 5.5 keV and 5.5 - 7 keV photon range, respectively. The calibration curves from Henke are used for the DEF film and x-ray crystal reflectivities. [12] Careful treatment of the fog and background and geometrical corrections for the curved crystal are taken into account in the data analysis. The resolution of the instrument is ~ 400.

The data for the 4 shots is summarized in the figure below where the conversion efficiency (CE) is plotted in figure 8 for the two positions for each shot as a function of laser energy. Both the 1 and 2 atm gas fill targets are shown for comparison. The circles represent the measurements from the axial view and taken overall cases, we observe a strong dependence on laser energy. The growth of conversion efficiency with laser energy is primarily due to the ability of the laser to penetrate the target and heat the gas. The squares represent measurements taken from the side view of the hohlraum and one of the points was obtained with only 5 beams from one side of the target. A comparison of the 1 atm case for the two different views shows that the side view is lower. In a shot with only 5 beams on one side, we find the measurement is roughly half of the 10 beam measurement, we believe the asymmetry is probably due to a combination of the volume of emission observed and the optical depth. Calculations do show a slight angular dependence, however, it is < 5 % and is not this pronounced. Measurements are now in progress to verify this angular dependence.

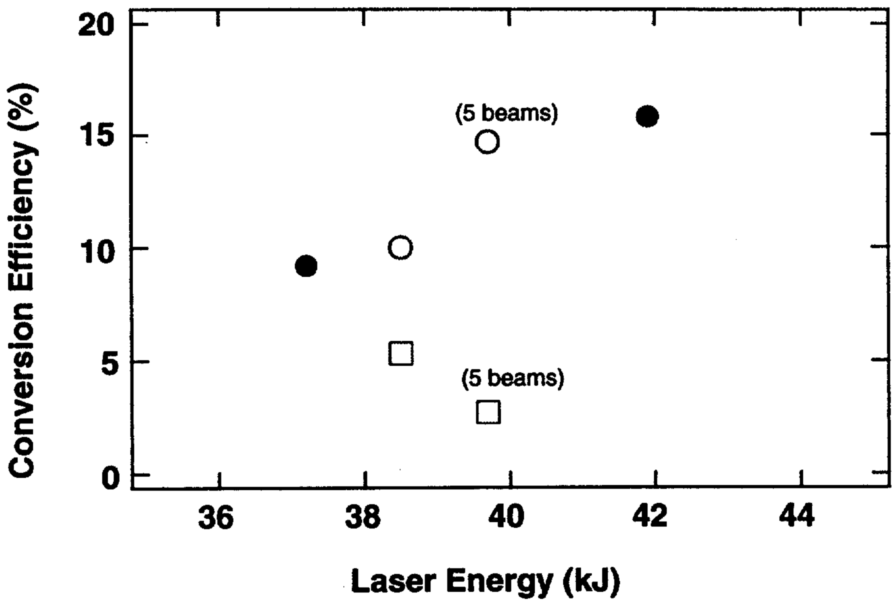

Figure 8. Conversion efficiency for Xe-filled Be hohlraum targets. The circles represent data for the axial view of the hohlraum. The squares represent the side view of the hohlraum. The side view has a generally lower conversion efficiency due to a combination of the volume of emission observed and optical depth effects. The symbols are empty for the 1 atm data and solid for the 2 atm data.

Finally, measurements were performed comparing backscatter for a beam with and without a kineform phase plate to determine if smoothing would increase conversion efficiency by lowering the backscatter. The phase plate did not have a significant effect on the SBS since the measurements were < 1.5 % SBS on all shots. It seemed to increase the SRS from 5% to 11 % in the two atmosphere gas targets.

4. SUMMARY

Experimental measurements have been performed on laser-produced plasmas which show they can produce a significant amount of hard x-rays above 4 keV. The target design was based on the use of an enclosure to keep the gas confined and at higher densities to prolong the x-ray pulse and enhance the production of x-rays from 4 to 7 keV which spans the Xe L-shell emission . We measure a conversion efficiency of 5 % - 15 %, depending on the angle of view, which is much larger than previous targets in this energy regime. This measurement is significantly higher than x-ray sources produced by laser irradiation of simple disk targets and may be greater than the those of gasbag targets.

These experiments showed that the laser did not sufficiently heat the center of the target and left a region from 250 to 500 µm long that did not emit. Recent modeling has shown that the ablation of the Be at the LEH significantly reduces the deposition of energy inside of the target. Future experiments will try to achieve higher conversion efficiencies in a longer pulse length.

ACKNOWLEDGEMENTS

We thank R. Kauffman for useful discussions and F. Ze for a relative calibration of the Bragg crystals used for the conversion efficiency measurement. We also thank the LUXEL Corp. for the production of the polyimide windows and assistance in target fabrication. This work was performed under the auspices of the U.S. Department of Energy by the Lawrence Livermore National Laboratory under Contract No. W-7405-ENG-48.

REFERENCES

[1]D. W. Phillion and C. J. Hailey, Phys. " Brightness and Duration of x-ray line sources irradiated with intense 0.53-μm laser light at 60 and 120 ps pulse width," Rev. A **34**, pp. 4886 - 4896, 1986.

[2]D. L. Matthews, E. M. Campbell, N. M. Ceglio, G. Hermes, R. Kauffman, L. Koppel, R. Lee, K. Manes, V. Rupert, V. W. Slivinsky, R. Turner, and F. Ze, "Characterization of laser-produced plasma X-ray sources for use in X-ray radiography," J. Appl. Phys. 54, pp. 4260-4268, 1983.

[3]W. Mead, E. M. Campbell, K. G. Estabrook, R. E. Turner, et al, "Laser irradiation of disk targets at 0.53 μm wavelength," Phys. Fluids 26, pp. 2316-2331, 1983.

[4]P. Alaterre, C. Popvics, J.-P. Geindre, J.-C. Gauthier, et al. "A study of the spectral emissions in laser-irradiated microdot targets at 0.53 and 0.27 μm wavelengths with micron resolution," Optics Commun. 49, pp. 140-145, 1984.

[5]S. G. Glendinning, P. Amendt, K. S. Budil, B. A. Hammel, et al., "Laser plasma diagnostics of dense plasmas," in Applications of Laser Plasma Radiation SPIE, vol.2523, (SPIE, Bellingham, WA, 1995), pp. 29-39.

[6]D. R. Kania, H. Kornblum, B. A. Hammel, J. Seely, et al, "Characterization of an x-ray-flux source for the production of high-energy-density plasmas," Phys. Rev. A 46, pp. 7853-68, 1992.

[7]P. Celliers, L. B. Da Silva, C. B. Dane, S. Mrowda, M. Norton, L. Hackel, D. Matthews, J. A. Abate, J. Maldonado, "Optimization of x-ray sources from a high-average-power Nd:glass Laser-produced plasma for proximity lithograph," Lawrence Livermore National Labortory annual report, UCRL-LR-105821-95-3, pp. 157-167.

[8]M. Chaker, B. La Fontaine, C. Y. Cote, J. C. Keiffer, et al, "Laser plasma sources for proximity printing or projection X-ray lithography," J.of Vacuum Sci. Technol. B **10**, pp. 3239-42, 1992.

[9]L. J. Suter, R. L. Kauffman, M. S. Maxon, J. F. Davis, "Efficient Production and Applications of 2- to 10-keV x-rays by Laser-Heated "underdense Radiatiors", Lawrence Livermore National Labortory annual report, UCRL-LR-105821-96-3, pp. 96.102, 1996.

[10]R. L. Kauffman, L. J. Suter, H. N. Kornblum, D. S. Montgomery, "X-ray production in Laser-Heated Xe gas Targets," Lawrence Livermore National Labortory annual report, UCRL-LR-105821-96-2, pp. 43 - 48, 1996.

[11]B. L. Henke, P. Lee, T. J. Tanaka, R. L. Shimabukuro, and B. K. Fujikawa, "Low-energy X-ray interaction coefficients: photoabsorption, scattering, and reflection-E=100-2000 eV, Z=1-94," At. Data Nucl. Data Tables **27**, p. 1-144, 1982.

[12] B. L. Henke, S. L. Kwok, J. Y. Yejio, H. T. Yamada, et al., "Low-energy X-ray response of photographic films. I. Mathematical models," J. Opt. Soc. B 1, pp. 818-827, 1984; B. L. Henke, F. G. Fujiwara, M. A. Tester, C. H. Dittmore, et al. "Low-energy X-ray response of photographic films. II. Experimental characterization," J. Opt. Soc B 1, pp. 828-49, 1984.

Technical Information Department • **Lawrence Livermore National Laboratory**
University of California • Livermore, California 94551